Journal of Diabetes and Metabolic Disorders; 2011; Vol 10, pp 1- 13

Evaluation of novel "biopaper" for cell and organ printing application: an *in vitro* study

Rana Imani[1], Shahriyar Hojjati Emami[1], Ali-Mohmmad Sharifi[3], Parisa Rahnama Moshtaq[1], Nafiseh Baheiraei[1], Hossein Fakhrzadeh[2]*

1. *Department of Biomedical Engineering, Amirkabir University of Technology, Tehran, Iran.*
2. *Endocrinology and Metabolism Research Center, Tehran University of Medical Sciences, Tehran, Iran.*
3. *Razi Institute for Drug Research and Department of Pharmacology, Tehran University of Medical sciences, Tehran, Iran.*

Abstract

Background: Recent advances in tissue engineering strategies have led to the development of the concept of tissue or organ printing-a biomedical application of rapid prototyping technology- that offers an interesting alternative to traditional solid scaffold-based tissue engineering. Biopaper is a bioprocessible biomimetic hydrogel that is specially designed for the bioprinting process.
Methods: In the present work, four different weight percentage ratios (100:0, 75:25, 50:50, 25:75) of agarose- gelatin blend hydrogels have been studied for the construction of biopaper for bioprinting application. Prepared hydrogels were characterized in terms of gel point temperature, mechanical stability, morphological observation, glucose diffusion, amount of in vitro degradation and cell viability. Tissue fusion study was performed on ChineseHamster Ovary cell aggregates embedded into the hydrogel.
Results: Based on obtained results, sol-gel transition point for samples with quite the same proportion of two components was in the physiological condition range (35-37°C). By adding gelatin content of hydrogels, the Young's modulus decreased about 4.5 times; furthermore, less dense network with larger pores resulted that provided glucose diffusion into hydrogels. Amount of degradation linearly decreased by enhancing agarose part of samples. Evaluation of tissue fusion process on sample of 50:50 demonstrated relative permissiveness of blend hydrogel with time scale of $\tau_{cc} = 60$ h.
Conclusion: Agarose-gelatin blend hydrogel with the same proportion of two components is capable to be used as a biopaper for bioprinting technology.

Keywords: Tissue engineering, Bio printing, Biopaper, Agarose, Gelatin, Tissue fusion process

***Corresponding Author:** Endocrinology and Metabolism Research Center, Tehran University of Medical Science, Shariati Hospital, North Kargar Street, 14114 Tehran, Iran. Tel: +98 (21) 88220037-38, Fax: +98 (21) 88220052, E-mail: emrc@tums.ac.ir

Introduction

Tissue engineering, design and fabrication of natural-like functional human tissues, is one of the multidisciplinary fields of biomedical engineering.Traditional tissue engineering is based on fabrication of porous solid biodegradable scaffolds with sequential cell seeding in bioreactors (1). Although scaffold- based tissue engineering has led to significant improvements in the reconstruction of various tissues and organs, there were some serious limitations included cell seeding, low level of precision in cell placement, vascularization of thick tissue construct, extremely laborious, slow and costly non-automated tissue assembly process (1). The design and manufacture of 3-D scaffolds with controlled and prescribed functionality can be readily achieved using computer aided tissue engineering techniques based on rapid prototyping methods (2,3). However, recent attempts using rapid prototyping technologies to design solid synthetic scaffolds suffer from the inability to precisely place cells or cell aggregates into a printed scaffold (4). These critical issues could be solved by cell and organ printing" technology that offers an interesting alternative to solid scaffold-based tissue engineering (5).

Organ printing could be defined as computer-aided 3-D tissue engineering of living organs based on the simultaneous deposition of cells and hydrogels with the principles of self-assembly (5). This new emerging technology has multiple roots that are classified in tree research areas: rapid prototyping, smart materials and cell adhesion (6). Bioprinting can be divided into three essential technological steps: pre-processing or development of design-files for organs, actual printing, and finally, post-processing or organ conditioning and accelerated tissue and organ maturation (5). This technology relies on developmental biology concepts named cellular self assembling and tissue fusion (7). Cellular self-assembly, the most fundamental mechanism in the origin of life and the evolution of complex biological organs, shows itself at all scales in living systems (8). By this mechanism, cells would attach each other and form three-dimensional (3D) spheroids. By tissue fusion, formed 3D spheroids or aggregates undergo fusion and make micro-tissues (7). Thus, based on insights from developmental biology, the proposed organ printing approach includes: precise computer-aided and controlled placement or deposition of cell aggregates; simultaneous deposition of cells and hydrogels; and utilization of the principles of biological self-assembly or fusion of cell aggregates. Using self-assembled cell aggregates as bioink in permissive stimuli-sensitive hydrogels as biopaper will dramatically accelerate tissue and organ assembly (5).

Design and synthesis of processible and biomimetic hydrogels (biopaper) represents one of the most important and challenging tasks in development of organ-printing technology (9). Biopaper can be defined as processible and biomimetic tissue fusion-permissive hydrogels specially designed for the bioprinting process (1). Organ printing extends the application of currently available hydrogels. In organ printing, hydrogels are used as support matrices. Hydrogels not only allow for easy processing with various rapid prototyping techniques, most of them are also suitable for entrapping living cells and therefore are popular as tissue engineering matrices (10).

Based on studies, it can be recognized that hydrogel is an essential biomatrix material for direct biofabrication using living cells, including inkjet biofabrication (9). The roles of hydrogel in bioprinting are recently reviewed in some papers (9, 10).

Up to now there are a few significant researches on Biopaper concept of bioprinting (11). Collagen as a common thermosensitive hydrogel has been used as a biopaper in various cell and organ printing (11, 12-15). In addition to collagen, agar (16), fibrin (15), alginate (17), pluronic (13), poly (N-isopropylacrylamide-co-2-(N, N-dimethylamino)- ethyl acrylate) copolymer (18) and polyacrylamide- based hydrogel (19) have been utilized. Studies have shown single polymer alone cannot meet different demands in tissue engineering in terms of both properties and performance. Blending is a simple method to combine the advantages of different polymers. The resulting polymer blends may show synergistic properties (20).

Agarose is one of the nontoxic, thermosensitive mechanically stable materials which have been well suited for biomedical application. However; its main drawback is low cell adhesiveness and cell proliferation as containing no moieties linked to cellular adhesion (10). On

the other hand, it is an ideal material for 3D plotting of scaffolds because the gel is stable at room temperature and 37 ºC, is not cell-toxic and exhibits adequate mechanical stability. The gelation process is fast and reliable and therefore easy to control. The gelation temperature is in the range of the temperature of an incubator which possibly allows incorporation of human cells into the 3D-plotting process in future. Its modification with peptides containing the cell recognition motif has attracted attention to increase the cell adhesiveness (21).

Gelatin is derived from denatured collagen and forms biocompatible hydrogels with cell - adhesive properties. Gelatin has a gelation temperature of 20ºC and forms a weak gel. The gel is not stable at 37 ºC (21). Previous studies on synthesis of agarose–gelatin conjugate have shown good results, making this combination an ideal candidate for tissue engineering, and cell enclosing capsules (22). As far as the authors are aware, no researches have been carried out to evaluate and characterized agarose-gelatin blend hydrogel as a biopaper for bioprinting application. In this study, we present a work on ability of agarose-gelatin hydrogel as a biopaper for application in cell and organ printing technology.

Methods

Preparation of Agarose-gelatin Blend Hydrogels

Gelatin powder (bovine skin type A, Aldrich, St Louis, MO), agarose powder (Boehringer, Germany) and distilled water were used to prepare four different agarose-gelatin blend hydrogels. Samples were prepared using different weight percent of agarose (100%, 75%, 50% and 25%). After dissolution and blending, liquid gels were casted into suitable mold until cooled, resulting in semisolid hydrogels. The obtained samples were then called AG100, AG75, AG50 and AG25, respectively (Table 1).

Gel point determination

Characterization of gel point of hydrogels was carried out with a universal dynamic rheometer (MCR300 SN599139, Paar-Physica, USA) to analyze the thermal behavior of hydrogels and to determine their gel points (21). The parallel plate geometry with a peltier element for temperature adjustment was set for deformation of 1% and an angular frequency of 1 Hz. The prepared solutions were placed between plates (95°C) and covered with silicon oil to prevent drying. Temperature was decreased from 95°C to 20°C and then increased to 95°C reversely. Storage modulus (G′) was continuously measured during the temperature variation (cooling and heating). Despite being near the gel point, the Storage modulus increased dramatically for all four solutions. Furthermore, complex viscosity of sol before gelation was determined.

Evaluation of mechanical stability

An indentation method was applied to calculate young's modulus (E) of gels in hydrated state. The deflection of hydrogel under static force by sphere indenter was measured. Briefly, hydrogel disks (3cm diameter and 1cm thickness) were prepared. Steel ball (110g, 30mm diameter for AG100, AG75 and AG50; 66.6 g, 22 mm for AG25), as an indenter, was placed slowly on the center of hydrogel disk. The height of the ball from the surface of the gel was determined with an accurate coulisse (0.1 mm graduation) after 120 s (Figure 1). Young's modulus may be determined from indentation with the Hertz equation (23):

$$E = \frac{3(1-\nu^2)F}{4h^{\frac{3}{2}}r^{\frac{1}{2}}} \qquad (1)$$

Where F represents the force of a sphere against the surface (dyne), h is the depth of indentation of a sphere (cm), r is the radius of the sphere (cm), and ν is Poisson's ratio that for swelled hydrogel was considered 0.5 (24). This procedure was repeated after immersion of prepared hydrogel in PBS in physiological condition (37ºC, pH 7.4) for 24 h.

Morphological Study of hydrogels

Internal porous structure of hydrogel was investigated by SEM. Briefly, prepared hydrogels were freezed at liquid nitrogen. Then, the frozen hydrogels were placed in a Petri dish, lyophilized with a freeze-dryer (ALPHA 1-2 LD, Germany) for 24 h in order to completely dry. The morphology of obtained sponge- like dried gels were observed using a scanning electron microscope (SEM, Tescan Vega 2XMU) after coating the samples with a thin

layer of gold under vacuum at 15 kV (Emitech K450X, England).

Glucose diffusion study

Agarose-gelatin hydrogel cylindrical samples (0.3ml) were prepared by a molding process into a 1ml syringe. Diffusion into the gel experiments consisted of placing a single hydrogel cylinder in a 10-mL screw-cap glass vial filled with a 7-mL PBS containing glucose (3 mg/mL). The samples were reserved at 37ºC and glucose concentration in surrounding medium was monitored by biochemical auto-analyzer (HIteck-LTD704) in different time steps (25).

Degradation study

Disk shaped hydrogels (1cm diameter, 0.5cm thickness) were prepared followed by immersing in to 10 ml PBS (37 ºC, pH 7.4) for 7 days and medium was replaced every day with fresh PBS. Samples were removed after one week and after freeze drying, changes in weight of dried hydrogels were monitored . Percent of degradation was measured by Equation (2):

$$\%D = \frac{W_{fn} - 0.03M_i}{0.03\,M_i} \times 100 \qquad (2)$$

Where, Wfn and Wi is final weight of samples after freeze-drying and initial weight of samples before immersing in PBS respectively.

Cell Viability analysis

Cell culture

Chinese Hamster Ovary cell (CHO) were obtained from Pasteur institute (Tehran, Iran) and maintained in RPMI1640 (Gibco) medium supplemented with 10% (v/v) fetal bovine serum (Gibco) and 1% penicillin-streptomycin (100 U/ml penicillin and 100 µg/ml streptomycin- Gibco) in a 90% humidified incubator of 5% CO2 in air at 37°C. The culture medium was changed every 48h, and the cells were sub-cultured every 2-3 days. Cells were harvested in sub-confluent stage, and cell suspension was prepared for subsequent analysis.

MTT Assay

Cytotoxicity of the blend hydrogels was determined by MTT (3-(3,4-dimethylthiazol-2-yl)-2,5-diphenyltetrazoliium bromide) assay (26). Briefly, 200 µL of cell suspension (25×103 cells/mL) was loaded in a 96-well cell culture plate and cultured for 24h.

Subsequently, the thin hydrogel films sized 1cm in diameter and 1mm in thickness were sterilized by UV and placed in wells (wells without films were served as a control). CHO cells at a density of about 25×103 cells/mL were seeded over the films. Following 72 h incubation, samples were carefully removed and incubated in culture medium containing 10 µL of MTT solution for 4 h. Then, absorbance of dimethyl solfoxide (DMSO) solution was measured at 590 nm using a micro plate reader (spectra count®). The percentage of relative growth rate (RGR) was calculated by dividing absorbance of samples to the absorbance of the control at 590 nm (Eq. 3) (27).

$$RGR = OD_e/OD_c \times 100 \qquad (3)$$

Where ODe and ODc are the average optical density value of the experimental and control sample, respectively.

Tissue fusion study

Preparing cellular aggregate

Based on our pervious study (28) hanging drop (HD) was used for preparation of cellular aggregates. Briefly, as HD culture technique, 20-µL drops of prepared cell suspension, containing approximately 5000 cells per drop, each were pipetted on the inner side of the lid of a 15 cm diameter tissue culture Petri dish respectively. After distribution of the drops, the lid was gently inverted and placed on the Petri dish, which contained 4mL PBS to humidify the culture chamber. Hanging drops were incubated under tissue culture conditions, allowing the cells to coalesce at the base of the droplets and to form aggregates.

Embedding procedure

Hydrogel disks of 10 mm diameter and 2 mm height were washed 3 times in RPMI to eliminate the storage medium. A 0.5 mm wide, 0.5 mm deep circular groove was cut into a disk, then filled with 2 contiguously placed aggregates. The groove was then refilled with gel to completely embed the aggregates (Figure 2). The structure was kept in incubator for 10 days at 37◦C and 5% CO2 in a tissue culture dish containing 10 ml of RPMI.

Imaging techniques

Aggregate structures in transparent agarose - gelatin gel were visualized on an Olympus IX-70 microscope at 4X magnification and images were captured with a Nikon CoolPix 5000 digital camera. Phase contrast microscopy images were taken on the constructs embedded in blend hydrogels during 9 days. The transparency of the hydrogel allowed using bright field microscopy to follow aggregate fusion. We defined as a measure of fusion the instantaneous value of the angle formed by two adjacent aggregates (29).

Statistical analysis

Results were presented as mean ± standard deviation (n=4). Each result was statistically analyzed by the independent sample t-test, using SPSS software 16.0. Statistical significance was set at $p<0.05$.

Results

Based on rheological data, obtained gel points of hydrogels are summarized in Table 2. Around sol gel transient point and polymer network formation, gel storage modulus will increase dramatically (Figure 3, a). To determine the gelling point of hydrogels more precisely, the first derivative of modulus (dG′) as a function of temperature (T) was plotted by MATLAB 7.0 (Figure 3, b). Peak of curve serves as the characteristic point of gelation. It can be seen that the gel point of AG50 and AG75 is near body temperature (35-37°C), making them more appropriate for plotting procedure. There was no sharp decreasing (as observed in cooling step) storage modulus during reverse heating around gel points for all samples (Figure 3, c).

The indentation test's results indicated a drop in E value after immersing PBS (Figure 4). By increasing gelatin content of hydrogels, acquired modulus decreased significantly due to weakness of gelatin network rather than agarose. Comparing swelling (after immersing) and non-swelling state (before immersing), for AG100 there was no drop in modulus while other samples lost their mechanical stability in vitro.

As SEM images depict, in pure agarose the hydrogel pores were small (<1 micron) and most of them were close-ended (Figure 5, a). Compared to AG100, AG75 had larger interconnected pores (Figure 5, b). Semi interpenetrated polymer networks of gelatin and agarose were significantly observed in AG50 structure (Figure 5, c).

Figure 6 represents the diffusion profiles of glucose over time at 37°C. Ct and C0 represent the glucose concentration at time of t and 0 in medium, respectively. The concentration of glucose in the solution (Ct) for all samples decreased till 210 min. For AG100, AG75 and AG50 decreasing manner was regular. Fluctuation of glucose concentration in solution for AG25 may be related to the fast gelatin releasing and loosing integrity of structure. AG50 provided slower diffusion of solute that followed by AG75.

Based on degradation study results (Figure 7), comparatively by adding gelatin components of the samples the amount of degradation elevated so that there were significant differences between all samples ($p<0.05$). AG25 lost nearly 60% of its initial own dry weight during 7 days. Considering negligible biodegradation of AG100, gelatin could be responsible for blend hydrogel biodegradation.

The cell viability results are displayed in Figure 8. Interestingly, RGR for AG50 was considerably higher than control at about 20% which proves an excellent cell-viability. The toxicity grade (CTG) of the samples is obtained by the relationship between RGR and CTG according to standard GB/T 16886-1997 (40). CTG of the AG100, AG75 and AG25 is grade 1 ($75<RGR<99$) indicating non-toxicity.

The transparency of agarose-gelatin blend hydrogel allows optically analyzing tissue fusion kinetic by following structure evolution (Figure 8, a-e). Figure 9 shows the time variation of the boundary between two adjacent aggregates. As aggregates joined together, the angle between the tangents to their boundaries (drawn from the point where they join) approached 130°. Two adjacent aggregates reached an approximate steady state after 9 day, which did not change in angle after 7 days of culture. The curve in Fig. 5 is an exponential fit to the data in the form $C(1-\exp(-t/\tau cc))$ that the quantity τcc defines a time scale of aggregate fusion. Acquired C and τcc based on fitted curve ($r2 = 0.996$) were 130.5 degree and 2.57 days respectively.

Table 1. Sample classification and compositions of hydrogels

Sample code	Gelatin(g)	Agarose(g)	Double distillated water
AG100	0.0000	0.0300	10.000
AG75	0.0075	0. 0225	10.000
AG50	0.0150	0.0150	10.000
AG25	0.0225	0.0075	10.000

Table 2. Gel point of blend hydrogels and complex viscosity of sol before gelation based on rheological study

Sample code	AG100	AG75	AG50	AG25
Estimated Gel point(°C)	39±0.3	37.1±0.8	35.2±0.5	28±1.5
Complex viscosity Before gelation (sol form) (Pa.s)	$1.25\pm0.1\times 10^{4}$	$1.75\pm0.08\times 10^{2}$	$1.63\pm0.1\times 10^{2}$	$9.34\pm0.12\times 10^{2}$

Fig 1. Indentation test set up for young's modulus measurement

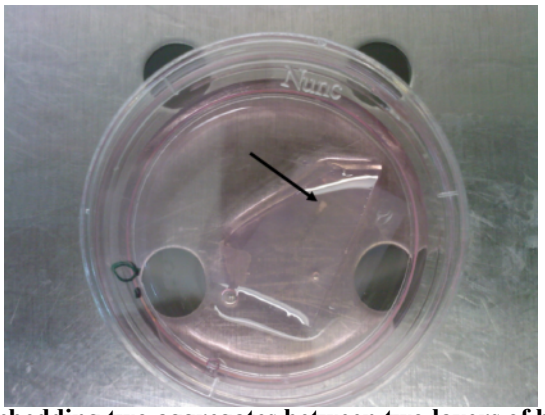

Fig 2. Embedding two aggregates between two layers of hydrogel. The arrow points embedded aggregates

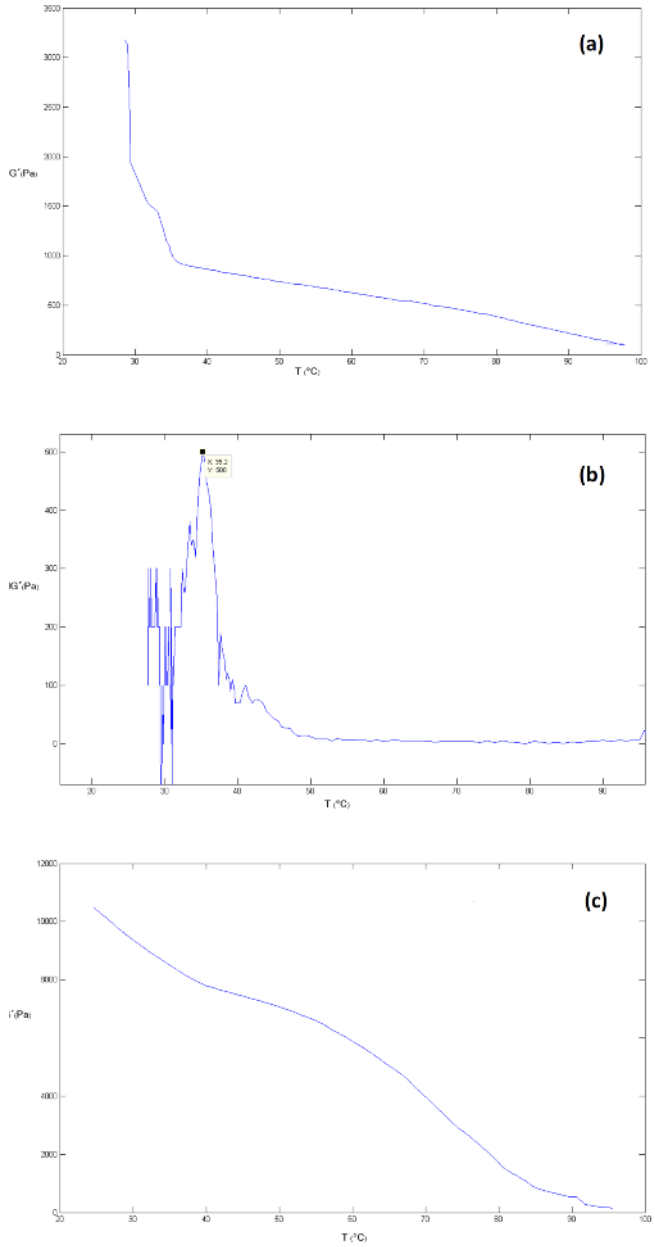

Fig 3. Curve of variation of storage modulus (cooling of sol) (a) and first derivative of storage modulus (b) variation of storage modulus (heating of gel) as a function of temperature (AG50)

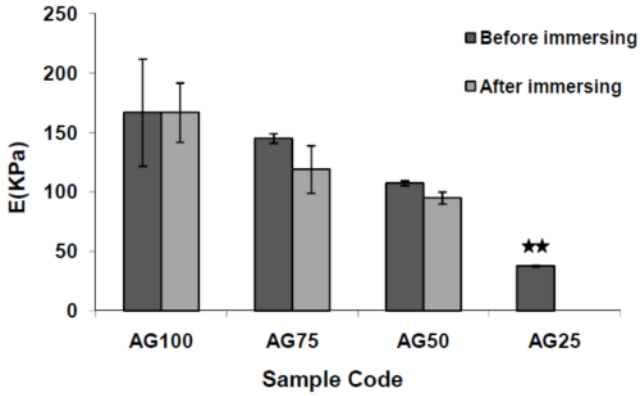

Fig 4. Comparison of Young's modulus of hydrogels obtained based on indentation test before and after immersing in PBS (37ºC, 24 h)

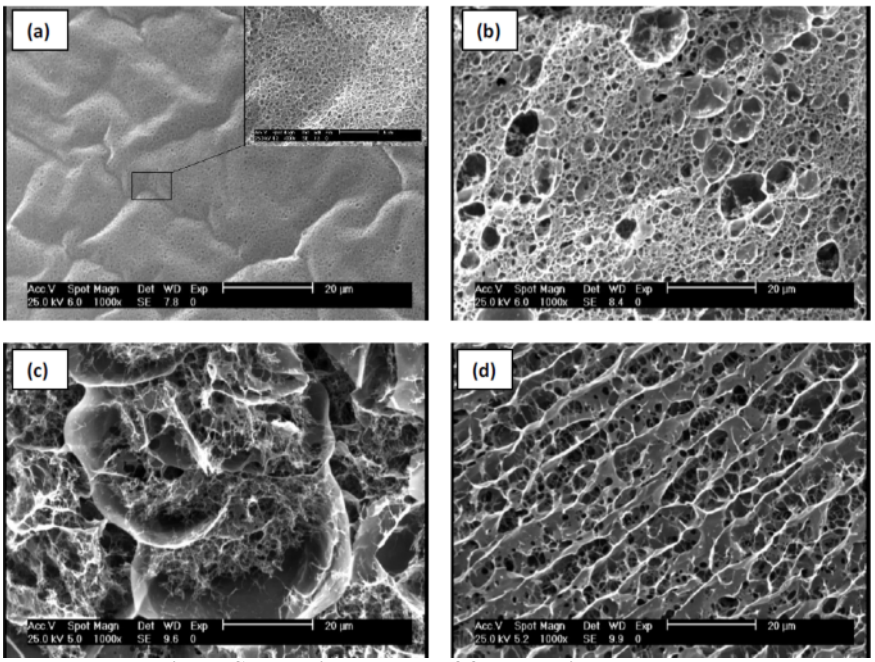

Fig 5. SEM micrograph of freeze dried hydrogels

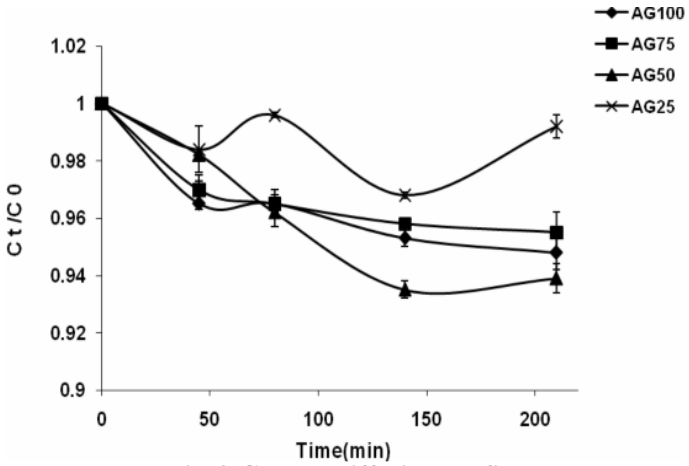

Fig 6. Glucose diffusion profile.

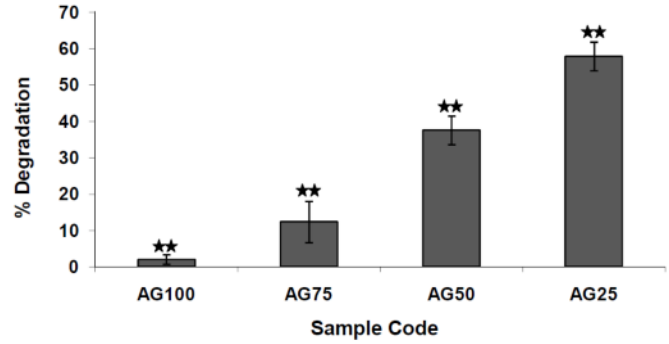

Fig 7. In vitro Degradation study of blend hydrogels after 7day, (indicates p<0.05)**

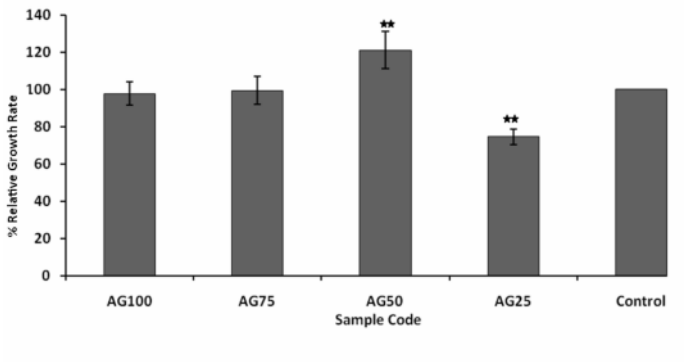

Fig 8. Relative growth rate of CHO cells based on MTT assay (indicates p<0.05)**

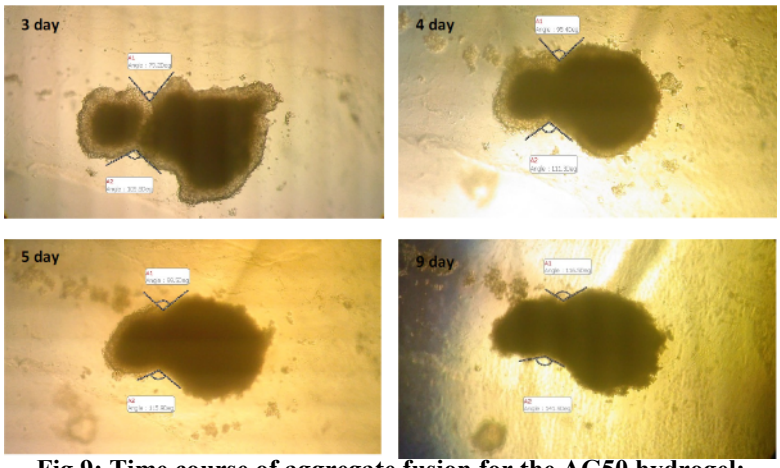

Fig 9: Time course of aggregate fusion for the AG50 hydrogel: Variation of the angle between two adjacent aggregates during 9 days

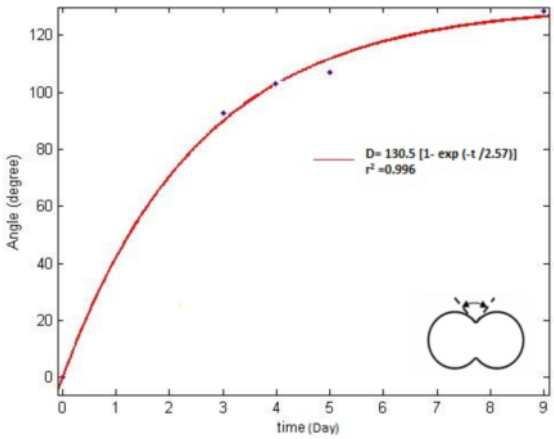

Fig 10. Angle measured between two tangential lines drawn to the point where the two aggregates join

Discussion

In this study, we have focused our attention to preparing and characterization of an appropriate blend hydrogel which could be applied as a biopaper for emerging cell and organ printing technology. Agarose and gelatin have been used for the construction of biopaper. The effects of blend composition on hydrogel properties (physical, mechanical and biological) were investigated.

One of the most important features of thermosensitive hydrogels as biopapers is their thermal behavior and the sol- gel transition temperature (19). Most of stimuli-sensitive hydrogels utilize sol–gel reactions based on photo /thermo/ chemical gelation phenomena, and have shown good potential for useful

hydrogels to construct 3D structures by computer based fabrication technologies like rapid prototyping (21,30,9,10). From a biopaper view point, the suitable hydrogel must be formed just after ejection of gel precursor ink, such as by decreasing temperature and immediate gel forming must occur. In addition, the gel precursor must have low viscosity for easy ejection by the inkjet device (9). So, determining and controlling gel point seems necessary in biopaper design as well as bioprinting device design. The cartridge and the medium temperature can be estimated from the temperature sweep experiments (21). Based on rheological data it can be proved that the gel point of AG50 and AG75 is near body temperature (35-37°C), making them more appropriate for plotting procedure. As mixing cells in to hydrogel solution should be done at some degree higher than the gel point, AG50 could be considered more desirable as a biopaper. That is, it causes less heating damage to cells during mixing till setting of hydrogel.

At present there are few methods available for characterizing the mechanical properties of hydrogel constructs: The tensile test or extensometry (31), unconfined compression test (32) and confined compression test (33).

Recently, indentation has been used as a new technique which enables the viscoelastic properties of hydrogels to be characterized more precisely (34). There are some advantages in this method, More importantly, the measurement can be performed for specimens that are fully immersed in solution or containing viable cells (34) that could be advantageous for tissue engineering applications (34,35,36). The indentation modulus is closely related to Young's modulus (*E*) and has been obtained from the slope of the force/indentation curve (37). In this study, Young's modulus of hydrogels was measured in equilibrium state (after 120 s contacting ball and gel) in two states: non-swelling and swelling for 24 h in physiological condition (37ºC, pH 7.4). Adding gelatin to the hydrogels result in dropping Young's modulus (from 166 KPa for pure agarose t0 38 KPa for AG25). Although most of samples provide more mechanical stability after immersing in PBS for 24 h under invitro condition, A25 undergoes rupture in indentation test. Decreasing E value was not statistically significant for AG50 and AG75 due to less biodegradation and more network density and chain entanglements.

Hydrogels are porous structures by nature due to high amounts of water against solid components. In tissue engineering application, interconnected pores play great roles in diffusion of nutrition or waste and cell migration. More porous internal structures provide better conditions for cell spreading and proliferation. The size of pores should be reasonable too. SEM images indicate less dens network with larger pores were produced by adding gelatin content of blend hydrogels. Interestingly interpenetrated networks of gelatin and agarose could be observed in AG50 structure**.** Comparing SEM outcomes, gelatin network is more porous than agarose and by blending these two polymers, the semi interpenetrated network could show various sizes of open pores.

Considering the use of blend hydrogel serving as the synthetic extracellular matrices (ECMs) for cells, it is important to understand the transport properties of blend hydrogels to predict if nutrients and waste products can freely be transported in to the matrix. Duo to importance of glucose as a main cell nutrient, glucose absorption was investigated. Typically, hydrogels are porous network on a scale of hundreds of micrometers through their 3D structure. Mass transport properties of the synthetic extracellular matrixes are key point to cell viability and nutrition. A successful hydrogel as a biopaper should allow rapid diffusion of nutrients, wastes, and important metabolic products. Le et.al (25) has reported the agarose hydrogels pore size about 450 A° for 2% concentration that it is appropriate for most of solute diffusion e.g. Glucose, albumin, vitamin B, etc. It is expected blending hydrogels and forming blend network changes pore size of pure ones. The molecular diffusion in the gel may be affected if the density or the complexity of the gel network is changed by the network structure (38).In terms of glucose diffusion, open porosity of AG50 permits glucose to diffuse freely, although the amount of absorbed glucose after 200 min does not differ remarkably. Regarding to SEM images (Figure 5), large and open pores of AG50 provide more and faster penetrating solutes, although there was no significant difference between AG75 and AG50 at 210 min.

As a construction of 3D cell containing structure, the hydrogel should have significant solid or viscoelastic properties to maintain 3D architectures. This support should be provided until the cells are assembled and maturated enough to support themselves (39). From bioprinting technique point of view, biodegradable biopaper should be designed as temporary support for post-printing tissue fusion and facilitate tissue formation by eliminating gradually. As degradation study demonstrated, the amount of degradation elevated by adding gelatin components of the samples. It is speculated that by loosing gelatin parts of blend hydrogel, density of the structure decreases and cellular migration in boundaries of the aggregates toward tissue fusion is facilitated, although agarose part could maintain and support strength and integrity of hydrogel during whole post-processing stage.

Biocompatibility is an important basis to be considered for any biomaterial. We analyzed the cell viability of blend hydrogels to CHO cells seeded on to tissue culture plates via MTT assay. The relative growth rate (RGR) of cells in the presence of samples was assessed (27). The results demonstrated the cell viability for most of the samples was above 90%, almost beyond compatibility. However, not surprisingly, AG25 had no desired outcome. It could be due to the fact that more degradation and released gelatin of this hydrogel could disturb cell environment.

Tissue fusion is a ubiquitous process during embryonic development (41) and constitutes the biological foundation for organ-printing technology (42). Although, few in vitro methods exist for the quantitative study of these processes and methods are needed to control them for applications in tissue engineering (43). Understanding and controlling tissue fusion is important for tissue engineering as they aim to build vascularized organs with complex shapes and multiple cell types (44).

Use of pre-formed cell aggregates that undergo fusion may be advantageous relative to individual cells due to high cell density, more ability to preserve their viability during handling procedures; reducing the time of making three-dimensional structures upon assembly (45).

In this report, we have utilized a simple and versatile assay to quantify fusion of two adjacent aggregates and used it to investigate the kinetic of tissue fusion process. The ideal hydrogel for cell aggregate printing must allow cells to survive and provide favorable conditions for post-printing self-assembly. In other words, ideal biopaper should be a tissue fusion- permissive hydrogel. The neighboring bio-ink droplets fuse and the bio-paper is eliminated by adding enzymes, changing temperature or secreting enzyme by enclosed cells. The success of bioprinting hinges on the capability of the bio-paper to gel rapidly enough to maintain the aggregates in the specified configuration but also slowly enough to allow continuity between successive layers (11).

The post printing cell rearrangements are highly dependent on the embedding gel, the "biopaper", whose composition could be controlled by the gel chemist (29). The behaviors of cells on or within the bio-paper are directed by cell–material interactions. Recently, it was demonstrated that the self-assembly and fusion of CHO aggregates embedded into 3D hydrogels depended greatly on the magnitude of cell–cell and cell–matrix interactions in the 3D systems. It was found, depending on the amount of cell adhesive ligands in the gel, that CHO aggregates either fused into a torodial 3D structure (when using RGD containing NeuroGel or 1.0 mg/ml collagen gel) or dispersed into the surrounding matrix (when using 1.7 mg/ml collagen gel). These findings could lead to the creation of functional bio-papers, especially when combined with other previous report of collagen printing (11). To study the feasibility of utilizing agarose-gelatin blend hydrogel as a biopaper for engineering 3D tissue constructs, we have manually printed (i.e., embedded) aggregates of living cells into gel (figure 2). Regarding other characteristics elucidated earlier, we selected AG50 as a more ideal biopaper for studying tissue fusion process.

Agarose and gelatin could provide facility for tissue fusion due to prevention of cell dispersion into scaffolds. agarose is non-adhesive for cells; so cell to cell interactions that drive tissue fusion predominate while an adhesive environment (e.g., collagen gel), where cell-to-ECM interactions influence the process has been shown to disassemble microtissues (46).

During measurements, we did not observe the collapse of the fused aggregates that, was less permissiveness than collagen (1 mg/ml) which means the aggregates need more time to reach equilibrium state of fusion ($\tau_{cc=}$ 60 h for blend hydrogel rather than $\tau_{cc=\ 24\ h}$ for 1 mg/ml collagen). In contrast, no undesirable cell spreading was observed in the outer boundaries of the aggregates. From other point of view, obtained C value (which indicates final angle between two adjacent aggregate) points out less contraction of printed patterns after tissue fusion as seen in figure 8, d.

Considering all results, it seems that agarose-gelatin blend hydrogel with selection of equal component concentration, AG50, is a feasible candidate to be utilized as a biopaper for cell and organ printing technology.

Acknowledgement

This study was funded by a grant provided from Endocrinology and Metabolism Research Center, Tehran University of Medical Sciences.

References

1. Mironov V, Kasyanov V, Markwald R. Bioprinting: Directed Self Assembly. *Chem Eng Prog* 2007; 103: 12-17.
2. Yeong WY. Rapid Prototyping in Tissue Engineering: Challenges and Potential. *Trends Biotechnol* 2004; 22: 643-650.
3. Hutmacher WD, Sittinger M, Risbud MV. Scaffold-Based Tissue Engineering: Rationale for Computer-Aided Design and Solid Free-Form Fabrication Systems. *Trends Biotechnol* 2004; 22: 354-362.
4. Mironov V, Boland T, Trusk T, et al. Organ Printing: Computer-Aided Jet-based 3D Tissue Engineering. *Trends Biotechnol* 2003; 21(4): 157-161.
5. Mironov V. Bioprinting: A Beginning. *Tissue Eng* 2006; 12: 631-634.
6. Mironov V, Beyond Cloning: Toward Human Printing. *The Futurist* 2003; 37: 34-36.
7. Marga F, Neagu A, Kosztin I, et al. Developmental Biology and Tissue Engineering. *Birth Defects Res* 2007; 81: 320–328.
8. Mironov V, Markwald R, Forgacs G. Organ Printing: Self Assembling Cell Aggregate as Cellular Aggregate Bioink. *Sci Med* 2003; 9: 69-71.
9. Nakamura M, Iwanaga S, Henmi C, et al. Biomatrices and biomaterials for future developments of bioprinting and biofabrication. *Biofabrication* 2010; 2: 1-6.
10. Federovich NE, Alblas J, Dewijn JR, et al. Review: Hydrogels as Extracellular Matrices for Skeletal Tissue Engineering: State-of-the-Art and Novel Application in Organ Printing. *Tissue Eng* 2007; 13: 1905-1925.
11. Jakab K, Neagu A, Mironov V, et al. Engineering Biological Structures of Prescribed Shape Using Self-assembling Multicellular Systems. *Proc Nat Aca Sci* 2004; 101: 2864–2869.
12. Roth EA, Xu T, Das M, et al. Inkjet Printing for High-Throughput Cell Patterning. *Biomaterials* 2004; 25: 3707–3715.
13. Jakab K, Damon B, Neagu A, et al. Three-Dimensional Tissue Constructs Built by Bioprinting. *Biorheo* 2006; 43: 509-513.
14. Jakab K, Norrote C, Damon B, et al. Tissue Engineering by Self-Assembly of Cells Printed into Topologically Defined Structures. *Tissue Eng Part A* 2008; 14: 413-21.
15. Xu T, Gregory CA, Molnar P, et al. Viability and Electrophysiology of Neural Cell Structures Generated By the Inkjet Printing Method. *Biomaterials* 2006; 27: 3580-3588.
16. Xu T, Jin J, Gregory C, et al. Inkjet printing of viable mammalian cells. *Biomaterials* 2005; 26: 93-99.
17. Boland T, Tao X, Damon B J, et al. Drop-on-demand printing of cells and materials for designer tissue construct. *Mat Sci Eng C* 2007; 27: 372–376.
18. Boland T, Mironov V, Gutowoska A, et al. Cell and Organ Printing 2: Fusion of Cell Aggregates in Three-Dimensional Gels. *Anat Rec A* 2003; 272:497–502.
19. Ilkhanizadeh S, Teixeira AI, Hermanson O. Inkjet printing of macromolecules on hydrogels to steer neural stem cell differentiation. *Biomaterials* 2007; 28: 3936–3943.
20. Liu J, Lin S, Li L, et al. Release of Theophylline from Polymer Blend Hydrogels. *Int J Pharm* 2005; 298: 117-125.
21. Landers R, Ubner H, Schmelzeisen U, et al. Rapid Prototyping of Scaffolds Derived from Thermoreversible Hydrogels and Tailored for Applications in Tissue Engineering. *Biomaterials* 2002; 23: 4437- 4447.
22. Sakai S, Hashimoto I, Kawakami K. Agarose–Gelatin Conjugate for Adherent Cell-Enclosing Capsules. *Biotechnol Lett* 2007; 29: 731–735.
23. Donnelly PI. *Mechanical Properties of Polymers*. New York, Wiley Interscience, 1971.

24. Ahearne M, Yang Y, Haj A. Characterizing the Viscoelastic Properties of Thin Hydrogel-based Constructs for Tissue Engineering Applications. *J R Soc Interface* 2005; 2: 455–463.
25. Li R, Altreuter D, Gentile F. Transport Characterization of Hydrogel Matrices for Cell Encapsulation. *Biotechnol Bioengin* 1996; 50: 365-373.
26. Lu HF, Targonsky ED, Wheeler MB, et al. Thermally Induced Gelable Polymer Networks for Living Cell Encapsulation. *Biotechnol Bioengin* 2007, 96: 146-155.
27. Wang M, Li Y, Wu J, et al. In vitro and In vivo Study to The Biocompatibility and Biodegradation of Hydroxyapatite/poly (vinyl alcohol)/ gelatin Composite. *J Biomed Mater Res A* 2008; 85: 418-426.
28. Sharifi AM, Imani R, Fakhrzadeh H, et al. Preparation of bioink for cell printing application: comparison of two 3D culture method, Hanging Drop and Conical Tube. *Iranian J Diabetes and Lipid Disorder* 2010; 9: 303-315.
29. Jakab K. Physical mechanism of cell rearrangements: from tissue liquidity to artificial organ structure. Ph.D. thesis, University of Missouri-Columbia, 2006.
30. Kwon IK, Matsuda T. Photo-polymerized microarchitectual constructs prepared by microstereolithography (μSL) using liquid acrylate-end-capped trimethylene carbonate-based prepolymers. *Biomaterials* 2004; 26: 1675-84.
31. Drury JL, Dennis RG, Mooney DJ. The tensile properties of alginate hydrogels. *Biomaterials* 2004; 25: 3187-3199.
32. Koob TJ, Hernandez DJ. Mechanical and thermal properties of novel polymerized NDGA-gelatin hydrogels. *Biomaterials* 2003; 24: 1285-1292.
33. Gu WY, Yao H, Huang CY, et al. New insight into deformation-dependent hydraulic permeability of gels and cartilage, and dynamic behavior of agarose gels in confined compression. *J Biomech* 2003; 36: 593–598.
34. Ahearne M, Yang Y, Haj A. Characterizing the Viscoelastic Properties of Thin Hydrogel-based Constructs for Tissue Engineering Applications. *J R Soc Interface* 2005; 2: 455–463.
35. Constantinides G, Kalcioglu Z, McFarland M. Probing Mechanical Properties of Fully Hydrated Gels and Biological Tissues. *J Biomech* 2008; 41: 3285–3289.
36. Gäbler S. Determination of the viscoelastic properties of hydrogels based on polyethylene glycol diacrylate (PEG-DA) and human articular cartilage. *Int J Materials Engineering Innovation*. 2009; 1: 3-20.
37. Hojjati Emami S, Salovey R. Crosslinked Poly (ethylene oxide) Hydrogels. *J App Poly Sci* 2003; 88: 1451-145.
38. Liu J. Lin S, Li L, et al. Release of Theophylline from Polymer Blend Hydrogels. *Int J Pharm* 2005; 298: 117-125.
39. Hutmacher DW. Scaffolds in tissue engineering bone and cartilage. *Biomaterials* 2000; 21: 2529-43.
40. Biological Evaluation of Medical Devices-Part 5: Tests for Cytotoxicity: In vitro methods. China Standard, GB/T 16886.5-1997.Issued in 11/04/2004.
41. Perez-Pomares JM, Foty RA. Tissue fusion and cell sorting in embryonic development and disease: biomedical implications. *Bioessays* 2006; 28:809-821.
42. Mironov V, Kasyanov V, Drake C, et al. Organ printing: promises and challenges. *Regen Med* 2008; 3: 93–103.
43. Rago AP, Dean DM, Morgan JR. Controlling Cell Position in Complex Heterotypic 3D Microtissues by Tissue Fusion. *Biotechnol Bioeng* 2009; 102: 231-1241.
44. Norotte C, Marga FS, Niklason LE, et al. Scaffold-free vascular tissue engineering using bioprinting. *Biomaterials* 2009; 30: 5910–5917.
45. Mironov V, Visconti RP, Kasyanov V, et al. Organ Printing: *Tissue Spheroids as Building Blocks*. *Biomaterials* 2009; 30: 1-11.
46. Napolitano AP, Chai P, Dean DM, et al. Dynamics of the self assembly of complex cellular aggregates on micromolded nonadhesive hydrogels. *Tissue Eng* 2007; 13: 2087-2094.